nature water

Article

https://doi.org/10.1038/s44221-024-00366-8

Unravelling groundwater–stream connections over the continental United States

Received: 30 December 2023

Accepted: 27 November 2024

Published online: 6 January 2025

Check for updates

Chen Yang [1,2,5] ✉, Laura E. Condon [3] ✉ & Reed M. Maxwell [1,2,4] ✉

Groundwater is a critical component of the terrestrial water cycle, yet the distance and depth of its connections with streamflow remain unquantified at large scale. Here we conducted a backward-particle-tracking simulation across the continental United States. We quantified the lateral length and vertical depth of groundwater flow discharged to streams as baseflow. Our simulation results suggest that water may travel longer distances underground before emerging in a stream than previously thought, and that deep groundwater sourced from consolidated sediments, aquifers typically 10–100 m below the ground surface, contribute more than half of the baseflow in 56% of the subbasins. Water-balance approaches may underestimate inter-basin groundwater flow due to concurrent groundwater exportation and importation of a watershed. Unexpectedly stronger connections of streamflow with deep and inter-basin groundwater flow paths found here have important implications for watershed resilience to climate change and persistence of contamination.

Groundwater is the largest accessible potable water store on our planet and its flow is critical in stabilizing the terrestrial hydrologic cycle, subsidizing (providing a stable source of water) streamflow and water for plants, especially during dry periods[1,2]. It is well established that groundwater residence times can be quite long[3] and are fractal in nature[4]. The distance and depth of groundwater flow paths (Fig. 1) are key characteristics of the hydrologic cycle and are important for parameterizing large-scale Earth system models[5]. This topic has been studied for more than a century[6–8], leading to the so-called Tóthian conceptualization of nested watersheds with local, intermediate and regional flow paths[9]. However, the lateral and vertical connections of groundwater flow to streams remain largely unknown[10–14].

Although the importance of lateral groundwater flow has been demonstrated in large-scale models that include groundwater–stream-flow and groundwater–land-surface interactions[1,2,15], approaches to trace the extent of and connections between groundwater and streams at the continental scale has previously remained out of reach. Prior work has studied long-distance, or inter-basin, groundwater flow using modelling and chemical tracers over limited spatial extents[16–21] or with quasi-analytical or water-balance-type approaches at larger scales[22,23]. Even with these limitations, many regional-scale studies suggest the prevalence of longer groundwater flow paths[24–26]. Observations of old water using tracers indicate that the circulation depth of groundwater may be hundreds of metres below the land surface, implying the contribution of deep groundwater to streamflow[10,27,28]. Despite these findings, most Earth system models still represent groundwater without lateral flow, and even critical zone observatories are limited to shallow subsurface[10,29–31]. Regional and local studies have provided many valuable insights, but due to their limited spatial extents, they are unable to fully capture the spectrum of the groundwater flow paths and their connections to surface water bodies. What is needed is a consistent analysis based on a comprehensive flow-particle-tracking

[1]Department of Civil and Environmental Engineering, Princeton University, Princeton, NJ, USA. [2]Integrated GroundWater Modeling Center, Princeton University, Princeton, NJ, USA. [3]Department of Hydrology and Atmospheric Sciences, University of Arizona, Tucson, AZ, USA. [4]High Meadows Environmental Institute, Princeton University, Princeton, NJ, USA. [5]Present address: School of Atmospheric Sciences, Sun Yat-sen University, Zhuhai, China. ✉e-mail: yangch329@mail.sysu.edu.cn; lecondon@arizona.edu; reedmaxwell@princeton.edu

https://doi.org/10.1038/s44221-024-00366-8

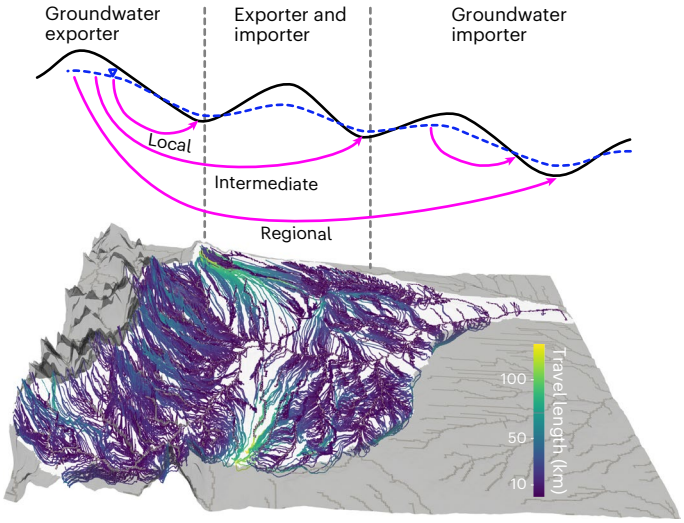

Fig. 1 | Here we quantify the extent of groundwater–stream connections over the continental United States. We combine the classical conceptual framework of nested groundwater flow systems (often called a Tóthian model[9]) with the simulation of particle tracking, shown here for the South Platte watershed, which has headwaters along the North American Continental Divide and travel lengths up to 130 km. Our goal is to identify the lateral length and vertical depth of a flow path, and if this flow path crosses watershed boundaries.

simulation at the continental scale, yet until now, this was limited by a lack of computationally efficient modelling platforms. The ability to do not only retrospective analyses but also predictive simulations that include potentially long groundwater flow paths to surface water is important for understanding water quality into the future[32].

In this work we combine the flow results of an integrated, continental-scale hydrologic model[33] and a Lagrangian particle-tracking model[34] that calculates flow paths and residence times over the contiguous United States. These results suggest that groundwater can flow hundreds of kilometres to emerge as streamflow, much longer than previously reported by tracer studies. Results also indicate that deep groundwater from consolidated sediments below the bedrock interface, not fully considered in models or observatories, play a larger role than previously thought.

The hydrologic model, ParFlow Continental United States (CONUS) 2.0[33], spans ~7.85 million km^2 (Supplementary Fig. 1a), covering the entire contiguous United States and portions of Canada and Mexico that contribute to transboundary flow. The CONUS 2.0 model has a depth of 392 m and a horizontal resolution of 1 km. Flow barriers (Supplementary Fig. 2 and Methods) were set at the bedrock depth (Supplementary Fig. 1b) to distinguish the unconsolidated and consolidated sediments and the correspondingly shallow and deep groundwater[29,35,36]. The CONUS 2.0 model dynamically simulates 3D groundwater flow through the entire domain, unsaturated flow and streamflow (Methods and related citations provide additional details on the model construction). Starting from a steady state 3D flow field generated by the CONUS 2.0 model, we then use the EcoSLIM model to track parcels of water using ~6 million particles. This mega annum (10^6 year) particle-tracking simulation leverages advances in computing, using parallel graphics processing units (GPUs), requiring the development of a new platform to efficiently use these resources[34,37,38].

Given the uncertainty inherent in groundwater simulations (particularly the subsurface configuration), a model evaluation was conducted. This evaluation is in two major phases: (1) the ParFlow CONUS 2.0 model results were compared to observations of water table depth and stream discharge and (2) the EcoSLIM particle-tracking results were compared to published estimates of groundwater age. This comparison is broadly summarized here, and more details are provided in Methods. As noted above the particle-tracking results rely on the flow field simulated by the ParFlow model. Thus, we first evaluate the flow field by comparing the ParFlow CONUS 2.0 model outputs to observations of streamflow and water table depth. This evaluation, published previously[33], showed good statistical performance comparing to over 635 K streamflow and water table depth observations (Methods). Whereas this evaluation builds confidence in the results, it must be acknowledged that uncertainties in these types of simulation still exist.

Particle-tracking results were directly evaluated by multiple datasets collected from prior studies[12,16,39–41]. The simulated groundwater age distribution compares favourably to that using mean ages of 1,279 samples collected from 21 principal aquifers[39] (abbreviated as 'measured', Fig. 2a) as indicated by the agreements of both peak ages and age ranges (Fig. 2b). Yet the simulated distribution captures age variations to much larger values. Simulated peak ages are also consistent with the average age of 14 macroscale basins (10 ± 5 years) summarized by Stewart et al.[40]. The simulated mean age and age range of each aquifer matches and expands the measured ones, respectively (Fig. 2c). More details of this comparison, and comparisons with other datasets, are in Methods. Whereas we have done our best to evaluate the model results with all available observations, it should be noted that direct particle-tracking studies are very limited. Our comparisons illustrate that the simulation is generating physically realistic results; however, it is impossible to fully validate the national-scale model.

Groundwater flow paths longer than 50 km are common

We divided the United States into roughly 40,000 subbasins based on drainage area, and each subbasin has an area around 100 km^2 comparable to the HUC12 (United States Geological Survey Hydrologic Unit Code) watershed[42]. For each subbasin, we calculated the lateral length as the average lateral length of all the flow paths in this subbasin (Methods). The lateral length of a groundwater flow path is defined as the lateral distance from the point of recharge to the point of discharge at a surface water body. Lateral lengths of subbasins range from <1 km to ~100 km (Fig. 3a). Lateral lengths longer than 50 km are common across the western United States (Fig. 3b), probably due to the dryer climate[16,22,43,44]. However, there are also areas with long flow paths along the Gulf Coastal Plain, Great Lakes and Atlantic Coastal Plain (Fig. 3b). This finding is consistent with local cases reported in prior studies[16,24–26,43,45]. Lateral lengths longer than 100 km are less frequent and occur mostly in the High Plains (Fig. 3c). The longest lateral length in the simulation is 238 km and occurs in the High Plains. This exceeds the observations of ~50 km in the Ordos Plateau in China[21] and ~100 km from the Andes to the Monte Desert in South America[19]. This work builds upon and extends these prior smaller-scale, individual studies by identifying all the long-distance groundwater flow paths within the CONUS using a consistent modelling framework.

Deep groundwater contributes substantially to streamflow

In addition to the lateral distance travelled from the point of recharge to the point of discharge, we also evaluated the maximum vertical depth that a parcel of water reaches on its journey (Fig. 3d). This quantity is an indication of the depth of active groundwater circulation. Similar to the lateral length of a subbasin, we calculated the vertical depth of a subbasin as the average depth of all the flow paths in a subbasin (Fig. 3d). Large depths more frequently happen in regions of steep topography gradients[12], such as the western United States and Appalachian ranges. Lateral length and vertical depth show similar spatial patterns (Fig. 3a,d), notably fragmented west of the High Plains and relatively uniform in the East.

We also evaluated the time spent in unconsolidated sediments above the flow barrier (shallow groundwater) and consolidated

https://doi.org/10.1038/s44221-024-00366-8

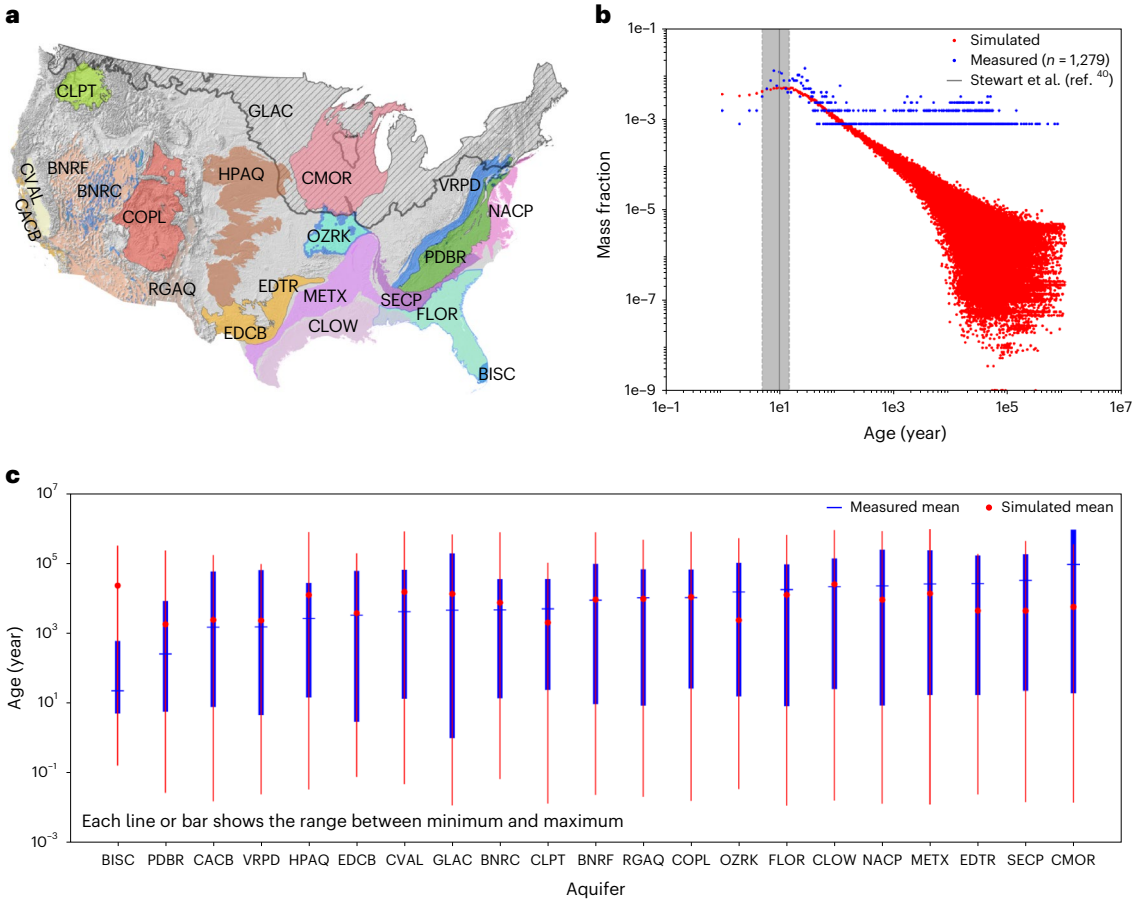

Fig. 2 | Simulated groundwater ages compare favourably to those reported in literature and expand understanding by providing a more complete age distribution of all aquifers. a, Locations of the 21 principal aquifers studied in Jurgens et al.[39]. **b**, Simulated groundwater age distribution agrees with that based on means of 1,279 samples from Jurgens et al.[39] (measured) at peak ages. The latter cannot capture the distribution of groundwater age at large values due to the limited number of samples. The average age of 14 macroscale basins summarized in Stewart et al.[40] is also indicated by the shaded grey line in **b**. Peak ages of three different data sources match each other well. **c**, The age range of each aquifer bracketed by minimum age and maximum age with the mean value indicated. Lines and bars are for simulated and Jurgens et al.[39], respectively. Simulated means compare well with that reported in Jurgens et al.[39], and simulated ranges bracket the reported ranges showing the expanded understandings. Panel **a** adapted from ref. 39 under a Creative Commons license CC BY 4.0. BISC, Biscayne; PDBR, Piedmont and Blue Ridge crystalline; CACB, California Coastal Basins; VRPD, Valley and Ridge and Piedmont and Blue Ridge carbonate; HPAQ, High Plains; EDCB, Edwards carbonate; CVAL, Central Valley; GLAC, Glacial; BNRC, Basin and Range carbonate; CLPT, Columbia Plateau basalts; BNRF, Basin and Range basin-fill; RGAQ, Rio Grande; COPL, Colorado Plateaus; OZRK, Ozark Plateaus; FLOR, Floridan; CLOW, Coastal Lowlands; NACP, Northern Atlantic Coastal Plain; METX, Mississippi Embayment and Texas Coastal Uplands; EDTR, Edwards and Edwards-Trinity; SECP, Southeastern Coastal Plain; CMOR, Cambrian-Ordovician.

sediments below the flow barrier (deep groundwater). Deep groundwater was commonly less focused due to its lumped representation or neglect in models and limited monitoring and sampling in observatories[5,10,11,46,47]. However, our simulation results suggest that most groundwater flow spends time in consolidated sediments as deep groundwater (Fig. 3e). A majority (56%) of the subbasins demonstrate contributions of deep groundwater greater than 0.5 (Fig. 3e). We further defined a ratio of the travel time in deep consolidated sediments to that in shallow unconsolidated sediments. Almost all subbasins (92%) show a travel time ratio larger than 1, indicating that groundwater spends more time moving through consolidated sediments than unconsolidated ones (Fig. 3f). Contribution fractions of deep groundwater are higher in the eastern United States (Fig. 3e,f).

Water-balance approaches systematically underestimate inter-basin groundwater flow

The ratio of stream discharge to watershed recharge (discharge ratio) is a common approach to quantify inter-basin groundwater flow[22,45]. This water-balance-based approach differentiates watersheds that export groundwater (where the discharge ratio is less than one) from those that import groundwater (where the discharge ratio is greater than one; Fig. 1). Here we identify groundwater exporters and importers two ways; first based on the discharge ratios calculated from our simulated water balance and second using particle tracking to directly calculate fluxes that cross watershed boundaries (Methods). We explore import and export behaviour by comparing the water balance and particle-tracking estimates of watershed groundwater discharge. If the water-balance approach agrees with particle tracking, plots of discharge ratios and import and export differences should agree.

For the subbasin watersheds examined here, we generally see disagreement between discharge ratios and import and export differences (Fig. 4a,b), indicating that water-balance approaches are not robust estimators of watershed import. Most subbasins export and import groundwater concurrently (Fig. 4c), and this behaviour cannot be captured by the discharge ratio alone. Our results suggest there are only 28 self-contained watersheds (0.07% of the domain), 1,572 groundwater exporters (3.97% of the domain) and 2,680 groundwater importers (6.77% of the domain) at the subbasin scale. In other words, inter-basin groundwater flow is ubiquitous over CONUS and much greater than previously evaluated by water-balance approach.

https://doi.org/10.1038/s44221-024-00366-8

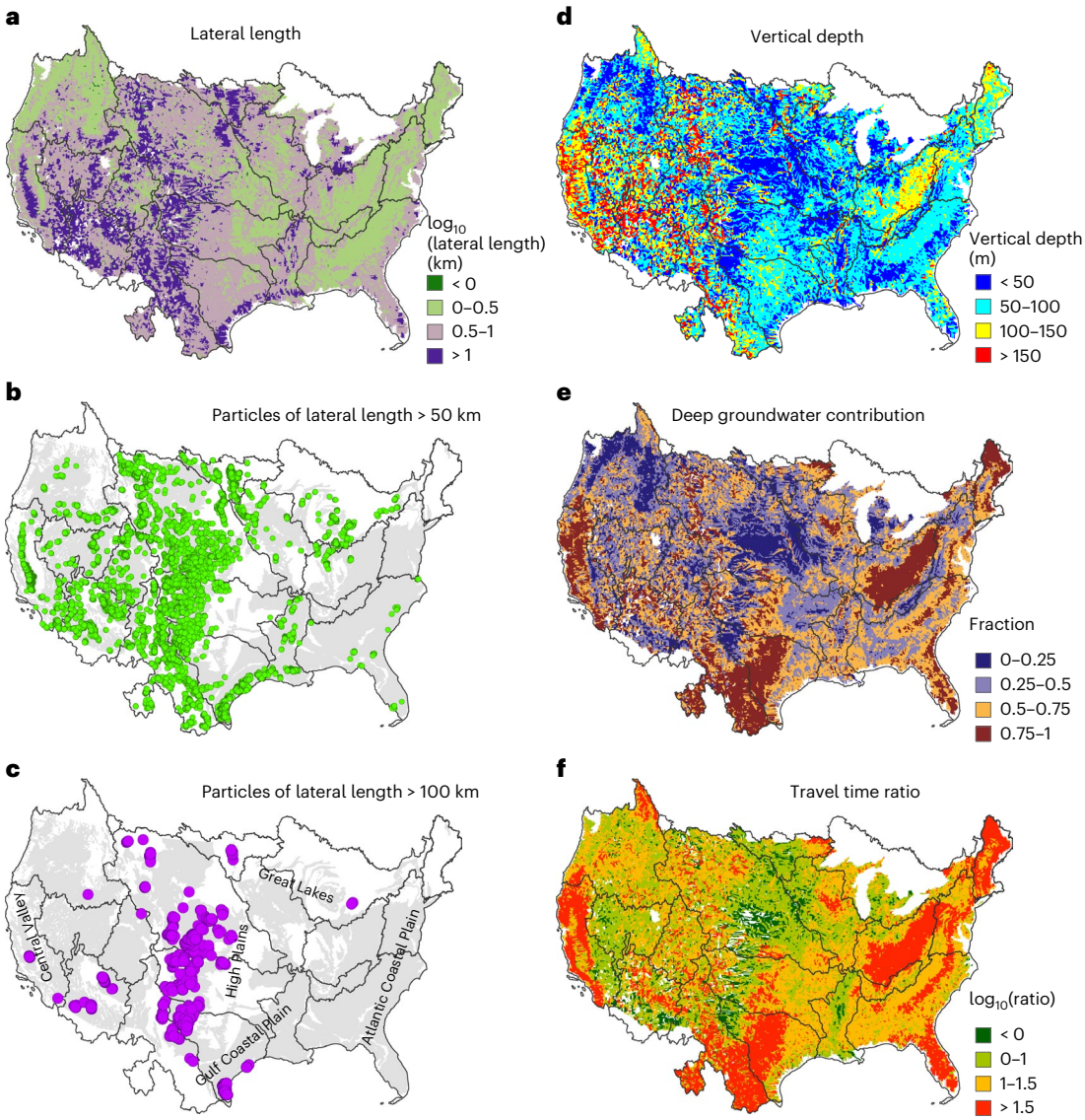

Fig. 3 | Lateral and vertical extents of groundwater flow in the continental United States. Groundwater of lateral lengths larger than 50 km are common, and deep groundwater from consolidated sediments substantially contributes to streamflow. **a**–**f**, This figure plots the lateral length from stream (discharge location) to land surface (recharge location) over CONUS (**a**), the discharge locations of particles with lateral length >50 km (**b**), the discharge locations of particles with lateral length >100 km (**c**), the vertical depth across CONUS (**d**), the fraction of deep groundwater to streamflow over CONUS (**e**) and the ratio of travel time in consolidated sediments to that in unconsolidated sediments spent by a flow path (**f**). Note that variables in **a** and **d**–**f** are averaged at the subbasin scale (Methods), grey lines are HUC2 watershed boundaries and grey areas in **b** and **c** are US major aquifers.

Groundwater connects nested watersheds, and only continental river systems may be treated in isolation

Our particle-tracking approach has the advantage of directly identifying inter-basin groundwater flow and accurately quantifying decreases in inter-basin flow with increasing watershed size. Inter-basin groundwater flow occurs in almost all watersheds at all four scales (subbasin to HUC2). The fraction of inter-basin exchange increases as the watershed-scale decreases. This would equate to water-balance errors of almost one-quarter (23.35%) at the subbasin scale, 8% at the HUC8 watershed scale, about 3% at the HUC4 watershed scale and less than 1% (0.81%) at the HUC2 or continental river basin (for example, Mississippi, Colorado) scale. This quantitative result with flow paths as the direct evidence confirms the hypothesis in previous studies[22,44] that watersheds at the subbasin scale studied here are 'leakier' whereas large watersheds such as HUC2 are more self-contained.

Understanding the length and depth of groundwater flow systems is central to understanding watershed dynamics. Still, the inherent difficulty of measuring groundwater residence times and the challenges of modelling large spatial scales have limited our ability to explore how groundwater flow systems change with scale. The extremely long lateral flow paths of groundwater discharged to streams (>200 km) and the substantial groundwater exchange between watersheds up to continental river systems suggest that it is inappropriate to use small watersheds as closed basic units in water resources management. Prior water-balance-based approaches have emphasized the role of inter-basin groundwater flow[44]. Our results suggest lateral exchanges between nested watersheds are much greater than previously thought as the concurrent exportation and importation of watersheds were not well identified. This further highlights the importance of lateral groundwater flow in the terrestrial water cycle and the need to model streams and aquifers as integrated systems across large scales.

https://doi.org/10.1038/s44221-024-00366-8

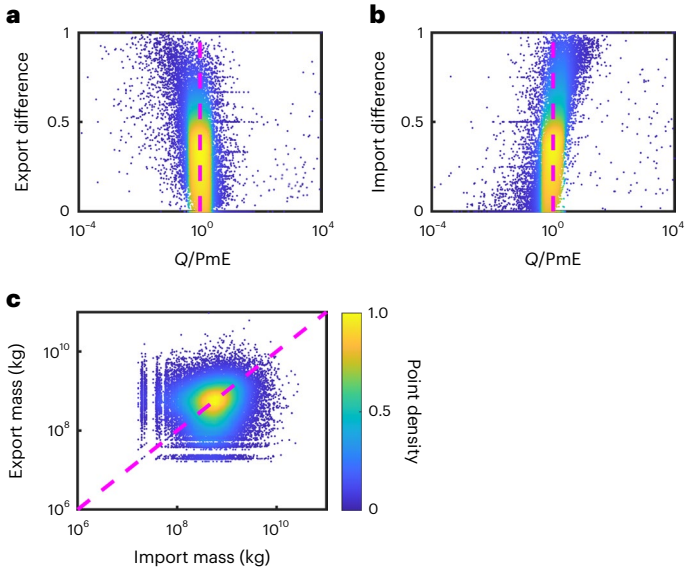

Fig. 4 | Water-balance approaches may misidentify groundwater exporters and importers and underestimate inter-basin groundwater because many watersheds are concurrent exporters and importers. a–**c**, Variations of export and import differences are plotted against the discharge ratio (**a**,**b**), and variations of export mass are plotted against import mass (**c**). The discharge ratio is the ratio of the streamflow discharge (*Q*) to the watershed recharge (that is, precipitation minus evapotranspiration, abbreviated as PmE). The discharge ratio was calculated using inputs and outputs of ParFlow (Methods). Export and import differences are calculated based on particle tracking (Methods). The export difference represents the fraction of local recharged particles finally discharged to other subbasins, whereas the import difference represents the contribution of particles from other subbasins to local streamflow discharge. All plots are at the subbasin scale, that is, each point representing a subbasin.

Whereas the work presented here represents the state of the art in simulating flow paths over the CONUS, we recognize that no simulation is perfect. In our estimation the largest uncertainties exist in the subsurface architecture, the recharge (for example, precipitation, P, minus evapotranspiration, ET, referred to as PmE) and the simulations of flow and particle tracking (for example, model resolution and number of particles). The huge computational expense of these simulations, and the lack of direct groundwater age observations, prevents a sensitivity and uncertainty analysis of the large-scale integrated hydrologic model and particle-tracking framework; a common challenge widely recognized by the large-scale groundwater modelling community[48]. However, throughout the ParFlow CONUS 2.0 model development process, the flow model along with major inputs were rigorously evaluated. The topography was evaluated compared to US Geological Survey (USGS) drainage areas[42], and an uncertainty analysis involving hundreds of integrated hydrologic simulations in representative large-scale watersheds constrained by observations were used to determine the final hydrostratigraphy[36,49]. The performance of both water table depth and streamflow of CONUS 2.0 were extensively evaluated, and improved performance was demonstrated relative to previous large-scale groundwater models[50]. Nevertheless, we recognize that these simulations are always subject to uncertainty that is often hard to quantify and that this uncertainty may be more noticeable at local scales where detailed heterogeneities unaccounted for in a continental-scale analysis are missing. Additionally, our ability to represent very small headwater systems is limited by the 1-km resolution of our model. Our results are not intended to be used for local mapping or to replace fine-scale models. Rather the purpose of the national simulations is to capture the distribution of behaviours across (1) large spatial scales and (2) a wide variety of hydrogeologic settings, not possible with local- or watershed-scale studies.

Our results suggest the extent of groundwater flow (both lateral lengths and vertical depths) across the CONUS is longer than previously understood and that deep groundwater may be more connected to streamflow than previously thought. Simulation results also provide insights into the circulation depth streamflow processes. The disproportionate contribution of solutes relative to discharge from groundwater to streams (that is, baseflow) has been widely recognized[16,51,52], controlling the quality of streamflow for important constituents such as legacy nitrate[53,54]. Our results further illustrate that a substantial quantity of streamflow is from deeper, consolidated sediments with longer deep travel times. These connections and pathways might be important to better understanding biogeochemical transformations and quantifying the global carbon and nitrogen cycles[55], and climate change[44,56,57]. Baseflow dominates the streamflow during dry periods, so our results highlight the impacts of deep groundwater on the quality of streamflow in the warming and drying climate, such as the more frequent droughts in recent years[58]. Deeper groundwater flow paths can be insulated from short-term climate variability and may help stabilize baseflow, but they can also transport contaminants and contribute to persistent water-quality issues. More work is needed to quantify these connections and their vulnerability to climate change, groundwater development and legacy contamination.

Methods

ParFlow CONUS 2.0 model

ParFlow simultaneously solves the three-dimensional variably saturated subsurface flow using the three-dimensional Richards' equation and two-dimensional overland flow using the shallow water equation[59]. ParFlow CONUS modelling platform currently has two models, that is, the early CONUS 1.0 model and the latest CONUS 2.0 model. CONUS 2.0 model is an improved version of the CONUS 1.0 model. CONUS 2.0 has the same 1-km horizontal resolution as CONUS 1.0 yet extends the CONUS 1.0 domain to coastlines, which increases the model area from 3,342 km × 1,888 km to 4,442 km × 3,256 km. CONUS 2.0 has improved hydrostratigraphy to better represent aquifers below soil horizons, which increases the total subsurface depth from 102 m of five layers to 392 m of ten layers.

Details are provided on the subsurface geology in 'Uncertainty analysis' below, but we briefly summarize the key points and the final CONUS 2.0 model configuration, which was used here. The subsurface was developed from a combination of publicly available datasets that tested both the datasets themselves and the conceptual models used to assemble them. In total, more than 80 subsurface configurations were evaluated, most using flow simulations that compared to observations. In all test cases, we keep the same vertical thickness and general layering structure. The ten layers have variable thicknesses of 200, 100, 50, 25, 10, 5, 1, 0.6, 0.3 and 0.1 m from bottom to top. The top four layers (2 m) are soils whereas the bottom six layers (390 m) represent hydrolithologies. In the final model configuration used for this analysis, the parameterization for the soil layers comes from the SSURGO dataset and the hydrolithologies come from the GLYMPHS dataset. In addition to this layering, we set flow barriers at the bedrock depth[29] in the CONUS 2.0 model to differentiate the shallow and deep groundwater in unconsolidated and consolidated sediments, respectively. The depth to bedrock in the baseline case is determined from the Shangguan et al.[29] dataset. Flow barriers are represented in the CONUS 2.0 model by multiplying the vertical hydraulic conductivity of the target cell interface by 0.001. Please refer to Supplementary Fig. 2 for the structure of CONUS 2.0. Then the model was driven by multi-year potential recharge to achieve a quasi-steady state.

Backward particle tracking

Backward particle tracking was conducted using the GPU-accelerated EcoSLIM[34,37,38] based on the inputs (porosities and depth of flow barriers) and outputs (saturations and three-dimensional velocities)

of the steady state CONUS 2.0 model. EcoSLIM is a Lagrangian particle-tracking model tracking the movement of particles through advection and molecular diffusion[60] in the subsurface. The travel information of particles, for example, travel time, travel length and flow path in the individual saturated or unsaturated zone and the entire subsurface, was recorded. The maximum depth of each particle's flow path was also identified in this study. Grid cells above and below the flow barriers were labelled one and two, respectively. Thus, the travel information of particles above and below the flow barriers could be distinguished. Two particles were put in each river cell at the top layer of the CONUS 2.0 model, generating ~6 million particles in total. Then the particles moved backward in the subsurface based on the reversed velocities until they reached the land surface, resulting in a total simulation time of ~1 million years.

Results analysis

Lateral length. The lateral length of a flow path, or the maximum lateral length (MLL) a particle can travel, was calculated using its horizontal coordinates by

$$\mathrm{MLL}_i = \sqrt{(x_{i,\mathrm{exit}} - x_{i,\mathrm{init}})^2 + (y_{i,\mathrm{exit}} - y_{i,\mathrm{init}})^2}, \quad (1)$$

where $x_{i,\mathrm{init}}$ and $x_{i,\mathrm{exit}}$ are the x coordinates of the ith particle at the initial and exit locations (that is, riverbed and land surface), and $y_{i,\mathrm{init}}$ and $y_{i,\mathrm{exit}}$ are the corresponding y coordinates.

The mass-weighted lateral length of each watershed at a given scale (that is, subbasin and different HUC levels) was calculated by averaging the lateral lengths of all particles initially located in this watershed through

$$\mathrm{MLL} = \frac{\sum_{i=1}^{i=N} \mathrm{MLL}_i \times m_i}{\sum_{i=1}^{i=N} m_i}, \quad (2)$$

where N is the total number of particles in the watershed, and m_i is the mass of the ith particle. The difference in particle mass is due to the spatially variable porosities along the riverbed, but the difference is small. We also calculated the recharge-weighted MLL and other metrics, but the difference was minor.

Vertical depth, deep groundwater contribution and travel time ratio. The maximum vertical depth (MVD), penetrating the flow barrier or not (PEN) and the travel time ratio (TTR) of each particle were obtained as follows: (1) the CONUS 2.0 model has $z = 0$ at the bottom. We recorded the smallest coordinate z of each particle path. The MVD for each particle was calculated as the model depth (392 m) minus the smallest coordinate z. (2) If a particle path crosses the flow barrier, it will have a travel time below the flow barrier larger than zero, which can be output directly from EcoSLIM. Thus, we labelled the particles penetrating the flow barrier by 1 and those not penetrating the flow barrier by 0 and defined this attribute as PEN. (3) A TTR of each particle was calculated using the travel time below the flow barrier in consolidated sediments divided by the travel time above the flow barrier in unconsolidated sediments.

The vertical length, deep groundwater contribution (percentage of particles penetrating flow barriers) and travel time ratio for each subbasin were calculated using equation (2) by replacing the MLL with MVD, PEN and TTR, respectively. The percentage of subbasins with a percentage of particles penetrating flow barriers greater than 50% is 56.20%, whereas that with a confined TTR greater than 1 is 91.61%.

Differences in import and export. We counted the particles with initial and exit locations in every watershed (N1 and N2). Given that backward particle tracking was conducted, N1 represents the particles discharged to rivers (that is, with initial locations in the watershed), whereas N2 represents the particles recharging the watershed (that is, with exit locations in the watershed). We also counted the particles with initial locations in a watershed and exit locations out of the watershed (N3), representing the particles imported into this watershed, and those with initial locations out of a watershed and exit locations in the watershed (N4), representing the particles exported from this watershed. Therefore, we have N2 (total recharged particles) − N4 (exported to other watersheds) + N3 (imported to this watershed) = N1 (total discharge to this watershed).

If N3 (imported) = N4 (exported) = 0, we identify this watershed as a self-contained watershed; if N3 (imported) > 0 and N4 (exported) = 0, we identify this watershed as a pure importer; if N4 (exported) > 0 and N3 (imported) = 0, we identify this watershed as a pure exporter; the remaining watersheds are then concurrent exporters and importers. At the subbasin scale, we identified 28 self-contained watersheds (0.07%), 2,680 pure importers (6.77%) and 1,572 pure exporters (3.97%), respectively. There are also 31 subbasins with N1 = N2 = 0, so the percentages were calculated by excluding these subbasins. Simultaneously, we define the mass of each portion (N1 to N4) as M1, M2, M3 and M4. M1 and M2 are the total recharged mass and total discharged mass of a watershed. M4 and M3 are the export and import masses used in Fig. 4c. We define the *export difference* as M4/M2 and the *import difference* as M3/M1 for each watershed, which were used in Fig. 4a,b. The export difference (M4/M2) represents the fraction of locally recharged particles finally discharged to other subbasins, whereas the import difference (M3/M1) represents the contribution of particles from other subbasins to local streamflow discharge.

Discharge ratio. We calculated the outflow (Q) at the outlet of each subbasin by Manning's equation[59,61] using the inputs (slopes in the x and y directions and Manning's roughness coefficients) and outputs (pressure head) of the CONUS 2.0 model. Multi-year averaged PmE is the input of CONUS 2.0 model, so we calculated the PmE for each subbasin by simply summing the PmE of grid cells located in the subbasin.

Model evaluation

ParFlow CONUS 2.0 model. The steady state CONUS 2.0 model was evaluated by comparing simulated water table depth (WTD) and streamflow with substantial observations; this process, whereas published elsewhere[33], is summarized here for completeness. Eighty-three thousand, four hundred seventy-one and 538,453 monitoring wells from USGS and Fan et al.[62] were used for WTD evaluation whereas 4,972 and 8,120 streamflow gauges from USGS and National Hydrography Dataset were used for streamflow evaluation, that is, 635,000 observations in total. Our evaluation is a 'distributed' approach covering the entire modelling domain (Fig. 3 in Yang et al.[33]) as opposed to the lumped approach limited to the outlet of a study domain addressed by Barclay et al.[63].

We used root mean standard deviation ratio (RSR) values of log-transformed WTDs to quantify the performance. RSR normalizes the Root Mean Squared Error using the standard deviation of observations; the smaller the RSR value, the better the model performance. We can see the obviously decreased RSR values of WTDs in majority of the HUC2 basins (Supplementary Fig. 3). A majority of the well comparisons showed good performance with RSR values of ~1.0. In general, the CONUS 2.0 model demonstrates better WTD performance than that of many global models[64]. In addition, improved streamflow from CONUS 1.0 to 2.0 was also observed in the evaluation as shown by the decreased RSR values, and about half of HUC2 basins showed excellent performance with RSR values smaller than 0.5. As streamflow simulated by ParFlow was automatically formed as opposed to predefining the stream channels, the improved performance of streamflow indicates the improved groundwater–surface-water partitioning, and thus reliable groundwater gradients essential for accurate particle tracking.

Particle tracking: baseflow age or travel time. The regions of simulated long-distance groundwater include those reported in previous studies[16]. Deeper travel depths were observed in the western United States and along the Appalachian ranges in our simulation results, consistent with the results reported by McIntosh and Ferguson[12], where they used water stable isotopes. Particle-tracking results were also evaluated by comparing the simulated groundwater ages with tracer-derived values collected from three previous studies[39–41], which showed good agreements and were detailed as follows.

The simulated ages of subbasins were calculated using equation (2), representing the travel times of baseflow. Travel time distributions of baseflow for four HUC2 basins are shown in Supplementary Fig. 4 because Stewart, et al.[40] reported the tritium-derived ages of baseflow in these HUC2s. The average age of 14 macroscale basins summarized by Stewart et al.[40] was also indicated in each subplot. In addition, the baseflow age of Copper Creek in the Upper Colorado River Basin reported by Carroll et al.[41] was indicated in Supplementary Fig. 4d as well. We see good agreement between the simulated peak ages and the tritium-derived ages. Discrepancies exist and may be caused by multiple factors. For example, tritium ages have the disturbances of agricultural activities, whereas our model represents a pre-development state; uncertainties also exist in the age dating using tritium.

We also compared our simulated ages with that of Jurgens et al.[39] using reverse modelling based on tracer concentrations. Our simulated age of each subbasin using equation (2) is an average of travel times along flow paths converged to this subbasin. Each flow path is a complete path starting from the riverbed and ending at the land surface. Due to the limited number of particles we used to balance the computation efficiency and resolution, we may not capture all the flow paths in the groundwater flow systems, which may cause some uncertainties in the ages. Groundwater ages reported in Jurgens et al.[39] were computed by the computer programme TracerLPM[65] using concentrations of multiple tracers (tritium, tritiogenic helium-3, sulfur hexafluoride, chlorofluorocarbons, carbon-14 and radiogenic helium-4) measured in wells or springs. We abbreviated this age as 'measured' hereinafter. Of the 1,279 sampling wells (10 of them are springs), 80% of them have depths greater than 60 m, and most of them have screen lengths greater than 20 m. As defined by the authors, the groundwater age they reported is the time water uses from their infiltration at the land surface to the sampling well. Hence, the age is an average of the travel times along part of the flow paths (that is, not complete paths). Also, these flow paths are a portion of all the paths in the aquifer system due to the limited well depths and screen lengths. Obviously, the ages we simulated and Jurgens et al.[39] reported have slightly different definitions, but both were obtained by largely sampling the groundwater flow paths in a given region, and thus, the old and young groundwater identified in a region, at least the pattern, should be largely consistent.

However, the simulated and 'measured' ages show unexpectedly great agreements. Quantified comparison by statistical metrics is shown in Fig. 2 in the main text, and here we show the comparison of spatial patterns (Supplementary Fig. 5). Older water is distributed in the eastern and southern coastal regions (for example, Texas-Gulf, South Atlantic Gulf and Mid-Atlantic), Lower Mississippi and part of the Upper Mississippi. Younger water is distributed along the Appalachian ranges. The western United States generally shows moderate ages relative to the extremely old and young waters in the eastern United States but is also scattered by very old and very young water. We see older water in the centre of the Pacific Northwest and younger water around. In eastern Upper Colorado (at about the junction of several HUC2s), both simulated and 'measured' ages are low. We can see similar places (1) at the junction of Missouri, Arkansas–White–Red and Upper and Lower Mississippi and (2) in the middle of the border between Texas-Gulf and Rio Grande, where both simulated and 'measured' ages are obviously small.

Uncertainty analysis

Hydrostratigraphy (that is, subsurface configuration) is important to the performance of ParFlow CONUS 2.0 model, including the model depth, layering, geologic types and hydraulic conductivities. To reduce the uncertainties of hydrostratigraphy, we tested more than 80 combinations of these components based on integrated hydrologic simulations using ParFlow-CLM. Soil layers were kept invariant during the test as the SSURGO soil data we used are generally an accepted and well-tested product. Tests were conducted over three large-scale basins of different climatic, topographic and geologic conditions, the Delaware–Susquehanna Basin, the Upper Colorado River Basin and the Little Washita Watershed. Hundreds of ParFlow-CLM runs were performed, and the performance of each run was evaluated by comparing the simulated water table depth and streamflow with USGS observations. Due to the expensive computational cost of large-scale hydrologic modelling, we did not conduct the common uncertainty/sensitivity analysis but treated this test work as an equivalence. Nevertheless, our test work is always absent in other large-scale hydrologic modelling. We briefly introduce the work here and refer to Tijerina-Kreuzer et al.[36] for details.

All runs in our tests were based on four subsurface structures (Supplementary Fig. 6). The first is homogeneous geology without flow barriers, the second is homogeneous geology with flow barriers at the bedrock depth, the third is bedrock layering under the bedrock depth but without flow barriers and the fourth is implementation of both bedrock layering and flow barriers. The bedrock layering here means one dataset of geology over another. Regarding the bedrock depth, there are two global datasets commonly accepted by the community, Pelletier et al.[66] and Shangguan et al.[29], with a maximum of 50 m and 540 m, respectively, and we adopted the latter one. Shangguan et al.[29] clarified that their dataset has a higher accuracy of depths smaller than 100 m. The majority of the bedrock depths in CONUS 2.0 are in 100 m (>90%; Supplementary Fig. 7), which is within the confidence interval of the Shangguan depth. Moreover, the larger limit of depths in Shangguan dataset is more consistent with the common recognition of the community (roughly 100–200 m) (ref. 10) although recent products are providing additional constraints on bedrock depth regionally[67]. To populate the geologic types, we employed the best available global datasets GLHYMPS 1.0 and 2.0 and the North America dataset from USGS. We know well that all datasets used in the model were not perfect, yet we have to move forward by assuming they represent the best community knowledge at current stage, which is a common way in large-scale hydrologic modelling[68].

Besides, we also tested different model depths (392 m and 1192 m), flow barriers at a constant depth of 192 m or the bedrock depth, the anisotropy of certain geologic types and *e*-folding describing the variations of hydraulic conductivity with slope and depth. We don't have specific configurations for other confining layers in CONUS 2.0, which are naturally represented by spatial variations of hydraulic properties. For example, the confining layers of lower permeabilities (for example, clay and loam) are well distinguished along river valleys (Supplementary Fig. 8). Finally, GLHYMPS 1.0 geologic types and the corresponding hydraulic conductivities with *e*-folding, together with the flow barriers at the bedrock depth showed the best overall performance over CONUS 2.0. Without flow barriers, it will result in too large baseflow. Note that the USGS geologic types did not show outstanding overall performances among others though the groundwater performance is comparable to GLHYMPS 1.0.

We recognize that the improved performance of the CONUS 2.0 model is not equivalent to the performance of particle tracking, yet it represents the best hydraulic gradients we have, which are essential for reliable particle-tracking results of lateral length and vertical depth. A prior study[44] summarized the major factors modulating the lateral distance of groundwater. The arid climate and high hydraulic conductivities could induce groundwater flow of long distance. Regarding the climate that we represented as PmE in CONUS 2.0, all uncertainties

directly come from the uncertainties of datasets. We tried to reduce these uncertainties by replacing the ~12 km resolution products[69] used in CONUS 1.0 to improved ~6-km resolution products[70] in CONUS 2.0. More importantly, Engdahl[71] showed the uncertainties of integrated hydrologic modelling is dominated by subsurface configuration as opposed to potential recharge.

Here we additionally analyse several most relevant uncertainties in particle-tracking results possibly induced by hydrostratigraphy. The baseline we refer to here is that we directly adopted geologic types of GLHYMPS 1.0, which describe the hydrolithologies of shallow subsurface roughly 100 m below the land surface. (1) If we do not set flow barriers at the bedrock depth, more flow paths can travel deeper than the bedrock depth, which will generate greater values of travel depth, deep groundwater contribution and deep travel time ratio. Obviously, groundwater flow of longer distance will increase due to the increased conductivities. (2) If we do not apply the *e*-folding technique, the higher hydraulic conductivities (especially higher at greater depths), relative to baseline would also generate the three vertical metrics and the lateral distance with greater values. (3) If we do not perform anisotropy of certain geologic types, which means higher vertical hydraulic conductivities in the corresponding regions, three vertical metrics and lateral distance of greater values will also be generated. Therefore, if we do not consider all the additional configurations in CONUS 2.0, more supportive results would be generated to our key points, that is, much more notable deep groundwater contribution to baseflow and longer lateral groundwater.

Data availability

Raw data of particle-tracking results and scripts for plotting used in this study are available via figshare at https://doi.org/10.6084/m9.figshare.24919938 (ref. 72).

Code availability

The ParFlow code used in this study is available via Zenodo at https://zenodo.org/records/7510554 (ref. 73). The EcoSLIM code used in this study is available via Zenodo at https://zenodo.org/records/7302297 (ref. 74).

References

1. de Graaf, I. E. M. & Stahl, K. A model comparison assessing the importance of lateral groundwater flows at the global scale. *Environ. Res. Lett.* **17**, 044020 (2022).
2. Maxwell, R. M. & Condon, L. E. Connections between groundwater flow and transpiration partitioning. *Science* **353**, 377–380 (2016).
3. Maxwell, R. M. et al. The imprint of climate and geology on the residence times of groundwater. *Geophys. Res. Lett.* **43**, 701–708 (2016).
4. Cardenas, M. B. Surface water–groundwater interface geomorphology leads to scaling of residence times. *Geophys. Res. Lett*. https://doi.org/10.1029/2008gl033753 (2008).
5. Fan, Y. et al. Hillslope hydrology in global change research and earth system modeling. *Water Resour. Res.* **55**, 1737–1772 (2019).
6. Dupuit, J. *Études Théoriques et Pratiques sur le Mouvement des Eaux dans les Canaux Découverts et à Travers les Terrains Perméables* (Dunod, 1863).
7. Forchheimer, P. Uber die Ergiebigkeit von Brunnenanlagen and Sickershlitzen. *Z. Archit. Ing. Ver.* **32**, 539–564 (1886).
8. Hubbert, M. K. The theory of ground-water motion. *J. Geol.* **48**, 785–944 (1940).
9. Toth, J. A theoretical analysis of groundwater flow in small drainage basins. *J. Geophys. Res.* **68**, 4795 (1963).
10. Condon, L. E. et al. Where is the bottom of a watershed? *Water Resour. Res.* **56**, e2019WR026010 (2020).
11. Fan, Y. Groundwater in the Earth's critical zone: relevance to large-scale patterns and processes. *Water Resour. Res.* **51**, 3052–3069 (2015).
12. McIntosh, J. C. & Ferguson, G. Deep meteoric water circulation in earth's crust. *Geophys. Res. Lett.* **48**, e2020GL090461 (2021).
13. Scanlon, B. R. et al. Global water resources and the role of groundwater in a resilient water future. *Nat. Rev. Earth Environ.* https://doi.org/10.1038/s43017-022-00378-6 (2023).
14. Jasechko, S., Kirchner, J. W., Welker, J. M. & McDonnell, J. J. Substantial proportion of global streamflow less than three months old. *Nat. Geosci.* **9**, 126–129 (2016).
15. Zeng, Y. et al. Global land surface modeling including lateral groundwater flow. *J. Adv. Model. Earth Syst.* **10**, 1882–1900 (2018).
16. Winter, T. C., Rosenberry, D. O. & LaBaugh, J. W. Where does the ground water in small watersheds come from? *Ground Water* **41**, 989–1000 (2003).
17. Modica, E., Burton, H. T. & Plummer, L. N. Evaluating the source and residence times of groundwater seepage to streams, New Jersey Coastal Plain. *Water Resour. Res.* **34**, 2797–2810 (1998).
18. Genereux, D. P., Nagy, L. A., Osburn, C. L. & Oberbauer, S. F. A connection to deep groundwater alters ecosystem carbon fluxes and budgets: example from a Costa Rican rainforest. *Geophys. Res. Lett.* **40**, 2066–2070 (2013).
19. Jobbagy, E. G., Nosetto, M. D., Villagra, P. E. & Jackson, R. B. Water subsidies from mountains to deserts: their role in sustaining groundwater-fed oases in a sandy landscape. *Ecol. Appl.* **21**, 678–694 (2011).
20. Gleeson, T. & Manning, A. H. Regional groundwater flow in mountainous terrain: three-dimensional simulations of topographic and hydrogeologic controls. *Water Resour. Res.* **44**, W10403 (2008).
21. Zhang, J. et al. Inflection points on groundwater age and geochemical profiles along wellbores light up hierarchically nested flow systems. *Geophys. Res. Lett.* **48**, e2020GL092337 (2021).
22. Schaller, M. F. & Fan, Y. River basins as groundwater exporters and importers: implications for water cycle and climate modeling. *J. Geophys. Res. Atmos.* **114**, D04103 (2009).
23. Worman, A., Packman, A. I., Marklund, L., Harvey, J. W. & Stone, S. H. Fractal topography and subsurface water flows from fluvial bedforms to the continental shield. *Geophys. Res. Lett.* **34**, L07402 (2007).
24. Williamson, A. K. & Grubb, H. F. *Ground-water Flow in the Gulf Coast Aquifer Systems, South-central United States* Report no. 1416F (U.S. Geological Survey, 2001).
25. Barlow, P. M. *Ground Water in Freshwater–Saltwater Environments of the Atlantic Coast* Report no. 1262 (U.S. Geological Survey, 2003).
26. Weeks, J. B., Gutentag, E. D., Heimes, F. J. & Luckey, R. R. *Summary of the High Plains Regional Aquifer-System Analysis in parts of Colorado, Kansas, Nebraska, New Mexico, Oklahoma, South Dakota, Texas, and Wyoming* Report no. 1400A (U.S. Geological Survey, 1988).
27. Humphrey, C. E. et al. Spatial variation in transit time distributions of groundwater discharge to a stream overlying the northern high plains aquifer, Nebraska, USA. *Water Resour. Res.* **60**, e2022WR034410 (2024).
28. O'Sullivan, A. M. et al. Effects of topographic resolution and geologic setting on spatial statistical river temperature models. *Water Resour. Res.* **56**, e2020WR028122 (2020).
29. Shangguan, W., Hengl, T., de Jesus, J. M., Yuan, H. & Dai, Y. J. Mapping the global depth to bedrock for land surface modeling. *J. Adv. Model. Earth Syst.* **9**, 65–88 (2017).
30. Cosgrove, B. et al. NOAA's national water model: advancing operational hydrology through continental-scale modeling. *JAWRA J. Am. Water Resour. Assoc.* **60**, 247–272 (2024).

31. Regan, R. S. et al. The U. S. Geological Survey National Hydrologic Model infrastructure: rationale, description, and application of a watershed-scale model for the conterminous United States. *Environ. Modell. Softw.* **111**, 192–203 (2019).
32. Ackerman Grunfeld, D. et al. Underestimated burden of per- and polyfluoroalkyl substances in global surface waters and groundwaters. *Nat. Geosci.* **17**, 340–346 (2024).
33. Yang, C., Tijerina-Kreuzer, D. T., Tran, H. V., Condon, L. E. & Maxwell, R. M. A high-resolution, 3D groundwater-surface water simulation of the contiguous US: advances in the integrated ParFlow CONUS 2.0 modeling platform. *J. Hydrology* https://doi.org/10.1016/j.jhydrol.2023.130294 (2023).
34. Yang, C. et al. Accelerating the Lagrangian particle tracking in hydrologic modeling to continental-scale. *J. Adv. Model. Earth Syst.* **15**, e2022MS003507 (2023).
35. Huscroft, J., Gleeson, T., Hartmann, J. & Börker, J. Compiling and mapping global permeability of the unconsolidated and consolidated earth: GLobal HYdrogeology MaPS 2.0 (GLHYMPS 2.0). *Geophys. Res. Lett.* **45**, 1897–1904 (2018).
36. Tijerina-Kreuzer, D. et al. Continental scale hydrostratigraphy: basin-scale testing of alternative data-driven approaches. *Groundwater* https://doi.org/10.1111/gwat.13357 (2023).
37. Yang, C., Maxwell, R. M. & Valent, R. Accelerating the Lagrangian simulation of water ages on distributed, multi-GPU platforms: the importance of dynamic load balancing. *Comput. Geosci.* **166**, 105189 (2022).
38. Yang, C. et al. Accelerating the Lagrangian particle tracking of residence time distributions and source water mixing towards large scales. *Comput. Geosci.* **151**, 104760 (2021).
39. Jurgens, B. C. et al. Over a third of groundwater in USA public-supply aquifers is Anthropocene-age and susceptible to surface contamination. *Commun. Earth Environ.* https://doi.org/10.1038/s43247-022-00473-y (2022).
40. Stewart, M. K., Morgenstern, U. & McDonnell, J. J. Truncation of stream residence time: how the use of stable isotopes has skewed our concept of streamwater age and origin. *Hydrol. Processes* **24**, 1646–1659 (2010).
41. Carroll, R. W. H., Manning, A. H., Niswonger, R., Marchetti, D. & Williams, K. H. Baseflow age distributions and depth of active groundwater flow in a snow-dominated mountain headwater basin. *Water Resour. Res.* **56**, e2020WR028161 (2020).
42. Zhang, J., Condon, L. E., Tran, H. & Maxwell, R. M. A national topographic dataset for hydrological modeling over the contiguous United States. *Earth Syst. Sci. Data* **13**, 3263–3279 (2021).
43. Gleeson, T., Marklund, L., Smith, L. & Manning, A. H. Classifying the water table at regional to continental scales. *Geophys. Res. Lett.* **38**, L05401 (2011).
44. Fan, Y. Are catchments leaky. *WIREs Water* **6**, e1386 (2019).
45. Condon, L. E. & Maxwell, R. M. Evaluating the relationship between topography and groundwater using outputs from a continental-scale integrated hydrology model. *Water Resour. Res.* **51**, 6602–6621 (2015).
46. Clark, M. P. et al. Improving the representation of hydrologic processes in Earth system models. *Water Resour. Res.* **51**, 5929–5956 (2015).
47. Shangguan, W., Dai, Y., Duan, Q., Liu, B. & Yuan, H. A global soil data set for earth system modeling. *J. Adv. Model. Earth Syst.* **6**, 249–263 (2014).
48. Gleeson, T. et al. GMD perspective: the quest to improve the evaluation of groundwater representation in continental- to global-scale models. *Geosci. Model Dev.* **14**, 7545–7571 (2021).
49. Swilley, J. S. et al. Continental scale hydrostratigraphy: comparing geologically informed data products to analytical solutions. *Groundwater* https://doi.org/10.1111/gwat.13354 (2023).
50. Maxwell, R. M., Condon, L. E. & Kollet, S. J. A high-resolution simulation of groundwater and surface water over most of the continental US with the integrated hydrologic model ParFlow v3. *Geosci. Model Dev.* **8**, 923–937 (2015).
51. Rumsey, C. A., Miller, M. P., Schwarz, G. E., Hirsch, R. M. & Susong, D. D. The role of baseflow in dissolved solids delivery to streams in the Upper Colorado River Basin. *Hydrol. Processes* **31**, 4705–4718 (2017).
52. Zhang, Y.-K. & Schilling, K. Temporal scaling of hydraulic head and river base flow and its implication for groundwater recharge. *Water Resour. Res.* https://doi.org/10.1029/2003WR002094 (2004).
53. Basu, N. B. et al. Managing nitrogen legacies to accelerate water quality improvement. *Nat. Geosci.* **15**, 97–105 (2022).
54. Van Meter, K. J., Van Cappellen, P. & Basu, N. B. Legacy nitrogen may prevent achievement of water quality goals in the Gulf of Mexico. *Science* **360**, 427–430 (2018).
55. Van Meter, K. J. & Basu, N. B. Time lags in watershed-scale nutrient transport: an exploration of dominant controls. *Environ. Res. Lett.* **12**, 084017 (2017).
56. Fan, Y. How much and how old. *Nat. Geosci.* **9**, 93–94 (2016).
57. Gleeson, T., Befus, K. M., Jasechko, S., Luijendijk, E. & Cardenas, M. B. The global volume and distribution of modern groundwater. *Nat. Geosci.* **9**, 161 (2016).
58. Miller, O. L. et al. How will baseflow respond to climate change in the Upper Colorado River Basin. *Geophys. Res. Lett.* **48**, e2021GL095085 (2021).
59. Kollet, S. J. & Maxwell, R. M. Integrated surface-groundwater flow modeling: a free-surface overland flow boundary condition in a parallel groundwater flow model. *Adv. Water Resour.* **29**, 945–958 (2006).
60. Maxwell, R. M., Condon, L. E., Danesh-Yazdi, M. & Bearup, L. A. Exploring source water mixing and transient residence time distributions of outflow and evapotranspiration with an integrated hydrologic model and Lagrangian particle tracking approach. *Ecohydrology* **12**, e2042 (2019).
61. Chow, V. T., Maidment, D. R. & Mays, L. W. *Applied Hydrology* (McGraw-Hill, 1988).
62. Fan, Y., Li, H. & Miguez-Macho, G. Global patterns of groundwater table depth. *Science* **339**, 940–943 (2013).
63. Barclay, J. R., Starn, J. J., Briggs, M. A. & Helton, A. M. Improved prediction of management-relevant groundwater discharge characteristics throughout river networks. *Water Resour. Res.* **56**, e2020WR028027 (2020).
64. Reinecke, R. et al. Importance of spatial resolution in global groundwater modeling. *Groundwater* **58**, 363–376 (2020).
65. Jurgens, B. C., Böhlke, J. K. & Eberts, S. M. *TracerLPM (Version 1): An Excel Workbook for Interpreting Groundwater Age Distributions from Environmental Tracer Data* Report no. 4-F3 (U.S. Geological Survey, 2012).
66. Pelletier, J. D. et al. A gridded global data set of soil, intact regolith, and sedimentary deposit thicknesses for regional and global land surface modeling. *J. Adv. Model. Earth Syst.* **8**, 41–65 (2016).
67. Goodling, P., Belitz, K., Stackelberg, P. & Fleming, B. A spatial machine learning model developed from noisy data requires multiscale performance evaluation: predicting depth to bedrock in the Delaware river basin, USA. *Environ. Modell. Softw.* **179**, 106124 (2024).
68. Fan, Y., Miguez-Macho, G., Weaver, C. P., Walko, R. & Robock, A. Incorporating water table dynamics in climate modeling: 1. water table observations and equilibrium water table simulations. *J. Geophys. Res. Atmos.* https://doi.org/10.1029/2006JD008111 (2007).

69. Maurer, E. P., Wood, A. W., Adam, J. C., Lettenmaier, D. P. & Nijssen, B. A long-term hydrologically based dataset of land surface fluxes and states for the conterminous United States. *J. Clim.* **15**, 3237–3251 (2002).
70. Livneh, B. et al. A spatially comprehensive, hydrometeorological data set for Mexico, the U.S., and Southern Canada 1950–2013. *Sci. Data* **2**, 150042 (2015).
71. Engdahl, N. B. Impacts of permeability uncertainty in a coupled surface–subsurface flow model under perturbed recharge scenarios. *Water Resour. Res.* **60**, e2023WR035975 (2024).
72. Yang, C., Condon, L. E. & Maxwell, R. M. Unraveling groundwater-stream connections at the continental scale. *figshare* https://doi.org/10.6084/m9.figshare.24263650.v1 (2023).
73. Smith, S. et al. parflow/parflow: ParFlow version 3.12.0. *Zenodo* https://doi.org/10.5281/zenodo.7510554 (2023).
74. Yang, C. EcoSLIM_CONUS. *Zenodo* https://doi.org/10.5281/zenodo.7302297 (2022).

Acknowledgements

This research has been supported by the US Department of Energy Office of Science (DE-AC02-05CH11231) and the US National Science Foundation Office of Advanced Cyberinfrastructure (OAC-2054506 and OAC-1835855) and Hydrologic Sciences (NSF-1805160) to C.Y., L.E.C. and R.M.M. The funders had no role in study design, data collection and analysis, decision to publish or preparation of the manuscript. We are pleased to acknowledge that the work reported on in this paper was substantially performed using the Princeton Research Computing resources at Princeton University, which is a consortium of groups led by the Princeton Institute for Computational Science and Engineering (PICSciE) and Office of Information Technology's Research Computing. We would like to acknowledge high-performance computing support from Cheyenne (https://doi.org/10.5065/D6RX99HX) provided by NCAR's Computational and Information Systems Laboratory, sponsored by the National Science Foundation.

Author contributions

C.Y. developed the methodology and conducted the formal analysis. C.Y., L.E.C. and R.M.M. conceptualized the study. L.E.C. and R.M.M. acquired the funds. C.Y., L.E.C. and R.M.M. wrote and approved the manuscript.

Competing interests

The authors declare no competing interests.

Additional information

Supplementary information The online version contains supplementary material available at https://doi.org/10.1038/s44221-024-00366-8.

Correspondence and requests for materials should be addressed to Chen Yang, Laura E. Condon or Reed M. Maxwell.

Peer review information *Nature Water* thanks Martin Briggs and the other, anonymous, reviewer(s) for their contribution to the peer review of this work.